Gluon and ghost propagators in the Landau gauge: Deriving lattice results from Schwinger-Dyson equations

A. C. Aguilar,[1] D. Binosi,[2] and J. Papavassiliou[1]

[1]*Departamento de Física Teórica and IFIC, Centro Mixto, Universidad de Valencia-CSIC, E-46100, Burjassot, Valencia, Spain*

[2]*European Centre for Theoretical Studies in Nuclear Physics and Related Areas (ECT*), Villa Tambosi, Strada delle Tabarelle 286, I-38050 Villazzano (TN), Italy*

(Received 14 February 2008; published 9 July 2008)

We show that the application of a novel gauge-invariant truncation scheme to the Schwinger-Dyson equations of QCD leads, in the Landau gauge, to an infrared finite gluon propagator and a divergent ghost propagator, in qualitative agreement with recent lattice data.

DOI: 10.1103/PhysRevD.78.025010 PACS numbers: 12.38.Lg, 12.38.Aw, 12.38.Gc

I. INTRODUCTION

The infrared sector of quantum chromodynamics (QCD) [1] remains largely unexplored, mainly due to the fact that, unlike the electroweak sector of the standard model, it does not yield to a perturbative treatment. The basic building blocks of QCD are the Green's (correlation) functions of the fundamental physical degrees of freedom, gluons, and quarks, and of the unphysical ghosts. Even though it is well known that these quantities are not physical, since they depend on the gauge-fixing scheme and parameters used to quantize the theory, it is widely believed that reliable information on their nonperturbative structure is essential for unraveling the infrared dynamics of QCD [2].

The two basic nonperturbative tools for accomplishing this task are (i) the lattice, where space-time is discretized and the quantities of interest are evaluated numerically, and (ii) the infinite set of coupled nonlinear integral equations governing the dynamics of the QCD Green's functions, known as Schwinger-Dyson equations (SDE) [3–5]. Even though these equations are derived by an expansion about the free-field vacuum, they finally make no reference to it, or to perturbation theory, and can be used to address problems related to chiral symmetry breaking, dynamical mass generation, formation of bound states, and other nonperturbative effects [1]. While the lattice calculations are limited by the lattice size used and the corresponding extrapolation of the numerical results to the continuous limit, the fundamental conceptual difficulty in treating the SDE resides in the need for a self-consistent truncation scheme, i.e., one that does not compromise crucial properties of the quantities studied.

It is generally accepted by now that the lattice yields in the Landau gauge (LG) an infrared finite gluon propagator and an infrared divergent ghost propagator. This rather characteristic behavior has been firmly established recently using large-volume lattices, for pure Yang-Mills (no quarks included), for both $SU(2)$ [6] and $SU(3)$ [7]. To be sure, lattice simulations of gauge-dependent quantities are known to suffer from the problem of the Gribov copies, especially in the infrared regime, but it is generally believed that the effects are quantitative rather than qualitative. The effects of the Gribov ambiguity on the ghost propagator become more pronounced in the infrared, while their impact on the gluon propagator usually stays within the statistical error of the simulation [8]. In what follows we will assume that in the lattice results we use the Gribov problem is under control.

In this article we show that the SDEs obtained within a new gauge-invariant truncation scheme furnish results (in the LG) which are in qualitative agreement with the lattice data. As has been first explained in [9], obtaining an infrared finite result for the gluon self-energy from SDEs, without violating the underlying local gauge symmetry, is far from trivial, and hinges crucially on one's ability to devise a self-consistent truncation scheme that would select a tractable and, at the same time, *physically meaningful* subset of these equations. To accomplish this, in the present work we will employ the new gauge-invariant truncation scheme derived in [10], which is based on the pinch technique [9,11] and its correspondence [12] with the background field method (BFM) [13].

II. SDES IN THE GAUGE-INVARIANT TRUNCATION SCHEME

The gluon propagator $\Delta_{\mu\nu}(q)$ in the covariant gauges assumes the form

$$\Delta_{\mu\nu}(q) = -i\left[\mathrm{P}_{\mu\nu}(q)\Delta(q^2) + \xi\frac{q_\mu q_\nu}{q^4}\right], \qquad (1)$$

where ξ denotes the gauge-fixing parameter, $\mathrm{P}_{\mu\nu}(q) = g_{\mu\nu} - q_\mu q_\nu/q^2$ is the usual transverse projector, and, finally, $\Delta^{-1}(q^2) = q^2 + i\Pi(q^2)$, with $\Pi_{\mu\nu}(q) = \mathrm{P}_{\mu\nu}(q)\Pi(q^2)$ the gluon self-energy. In addition, the full-ghost propagator $D(p^2)$ and its self-energy $L(p^2)$ are related by $iD^{-1}(p^2) = p^2 - iL(p^2)$. In the case of pure (quarkless) QCD, the new SD series [10] for the gluon and ghost propagators reads (see also Fig. 1)

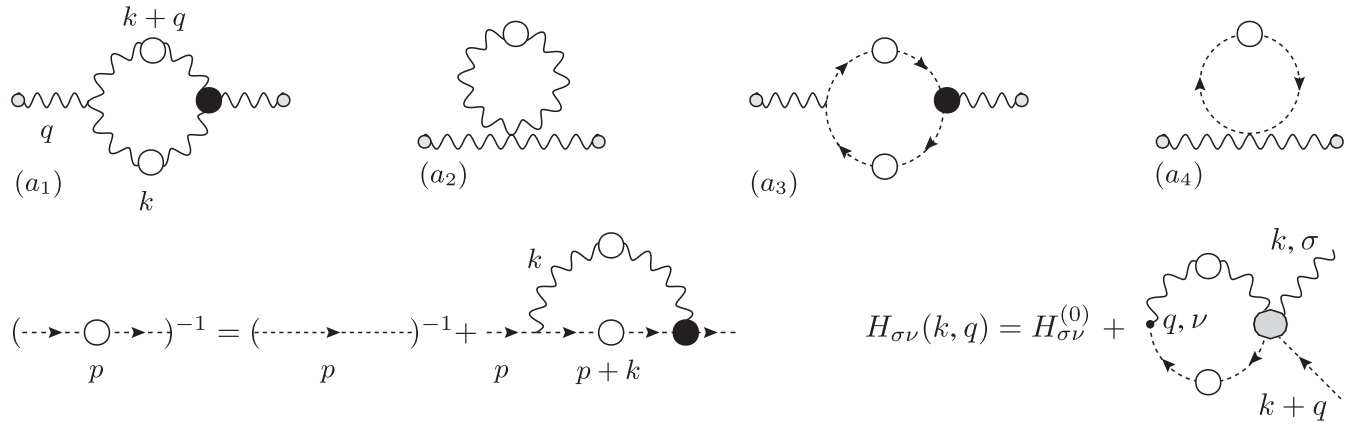

FIG. 1. The new SDE for the gluon-ghost system. Wavy lines with white blobs are full gluon propagators, dashed lines with white blobs are full-ghost propagators, black blobs are full vertices, and the gray blob denotes the scattering kernel. The circles attached to the external gluons denote that, from the point of view of Feynman rules, they are treated as background fields.

$$\Delta^{-1}(q^2)\mathrm{P}_{\mu\nu}(q) = \frac{q^2\mathrm{P}_{\mu\nu}(q) + i\sum_{i=1}^{4}(a_i)_{\mu\nu}}{[1+G(q^2)]^2},$$
$$iD^{-1}(p^2) = p^2 + i\lambda\int_k \Gamma^\mu \Delta_{\mu\nu}(k)\mathbf{\Gamma}^\nu(p,k)D(p+k),$$
$$i\Lambda_{\mu\nu}(q) = \lambda\int_k H^{(0)}_{\mu\rho}D(k+q)\Delta^{\rho\sigma}(k)H_{\sigma\nu}(k,q), \quad (2)$$

where $\lambda = g^2 C_\mathrm{A}$, with C_A the Casimir eigenvalue of the adjoint representation [$C_\mathrm{A} = N$ for $SU(N)$], and $\int_k \equiv \mu^{2\varepsilon}(2\pi)^{-d}\int d^dk$, with $d = 4-\epsilon$ the dimension of space-time. Γ_μ is the standard (asymmetric) gluon-ghost vertex at tree level, and $\mathbf{\Gamma}^\nu$ the fully-dressed one. $G(q^2)$ is the $g_{\mu\nu}$ component of the auxiliary two-point function $\Lambda_{\mu\nu}(q)$, and the function $H_{\sigma\nu}$ is defined diagrammatically in Fig. 1. $H_{\sigma\nu}$ is in fact a familiar object [1]: it appears in the all-order Slavnov-Taylor identity (STI) satisfied by the standard three-gluon vertex, and is related to the full gluon-ghost vertex by $q^\sigma H_{\sigma\nu}(p,r,q) = -i\mathbf{\Gamma}_\nu(p,r,q)$; at tree level, $H^{(0)}_{\sigma\nu} = ig_{\sigma\nu}$.

When evaluating the diagrams (a_i) one should use the BFM Feynman rules [13]; notice, in particular, that (i) the bare three- and four-gluon vertices depend explicitly on $1/\xi$, (ii) the coupling of the ghost to a background gluon is *symmetric* in the ghost momenta, (iii) there is a four-field coupling between two background gluons and two ghosts. Thus, for the gluonic contributions we find

$$(a_1)_{\mu\nu} = \frac{\lambda}{2}\int_k \tilde{\Gamma}_{\mu\alpha\beta}\Delta^{\alpha\rho}(k)\tilde{\mathbf{\Gamma}}_{\nu\rho\sigma}\Delta^{\beta\sigma}(k+q),$$
$$(a_2)_{\mu\nu} = \lambda g_{\mu\nu}\int_k \Delta^\rho_\rho(k) + \lambda\left(\frac{1}{\xi}-1\right)\int_k \Delta_{\mu\nu}(k), \quad (3)$$

with $\tilde{\Gamma}^{\mu\alpha\beta}(q,p_1,p_2) = \Gamma^{\mu\alpha\beta}(q,p_1,p_2) + (p_2^\beta g^{\mu\alpha} - p_1^\alpha g^{\mu\beta})\xi^{-1}$, $\Gamma_{\mu\alpha\beta}$ the standard QCD three-gluon vertex, and $\tilde{\mathbf{\Gamma}}_{\mu\alpha\beta}$ is the fully-dressed version of $\tilde{\mathbf{\Gamma}}_{\mu\alpha\beta}$. For the ghost contributions, we have instead

$$(a_3)_{\mu\nu} = -\lambda\int_k \tilde{\Gamma}_\mu D(k)D(k+q)\tilde{\mathbf{\Gamma}}_\nu,$$
$$(a_4)_{\mu\nu} = 2\lambda g_{\mu\nu}\int_k D(k), \quad (4)$$

with $\tilde{\Gamma}_\mu(q,p_1,p_2) = (p_2-p_1)_\mu$, and $\tilde{\mathbf{\Gamma}}_\mu$ its fully-dressed counterpart. Because of the Abelian all-order Ward identities (WIs) that these two full vertices satisfy (for all ξ), namely $q^\mu\tilde{\mathbf{\Gamma}}_{\mu\alpha\beta} = i\Delta^{-1}_{\alpha\beta}(k+q) - i\Delta^{-1}_{\alpha\beta}(k)$ and $q^\mu\tilde{\mathbf{\Gamma}}_\mu = iD^{-1}(k+q) - iD^{-1}(k)$, one can demonstrate that $q^\mu[(a_1)+(a_2)]_{\mu\nu} = 0$ and $q^\mu[(a_3)+(a_4)]_{\mu\nu} = 0$ [14].

For the rest of the article we will study the system of coupled SDEs (2) in the LG ($\xi = 0$), in order to make contact with the recent lattice results of [6,7]. This is a subtle exercise because one cannot set directly $\xi = 0$ in the integrals on the right-hand side (rhs) of (3), due to the terms proportional to $1/\xi$. Instead, one has to use the expressions for general ξ, carry out explicitly the set of cancellations produced when the terms proportional to ξ generated by the identity $k^\mu\Delta_{\mu\nu}(k) = -i\xi k_\nu/k^2$ are used to cancel $1/\xi$ terms, and set $\xi = 0$ only at the very end. It is relatively easy to establish that only the bare part $\tilde{\Gamma}_{\nu\alpha\beta}$ of the full vertex contains terms that diverge as $\xi \to 0$. Writing $\tilde{\mathbf{\Gamma}}_{\nu\alpha\beta} = \tilde{\Gamma}_{\nu\alpha\beta} + \tilde{\mathbf{K}}_{\nu\alpha\beta}$, we thus have that $\tilde{\mathbf{K}}_{\nu\alpha\beta}$ is regular in that limit, and we will denote by $\mathbf{K}_{\nu\alpha\beta}$ its value at $\xi = 0$. Introducing $\Delta^\mathrm{t}_{\mu\nu}(q) = \mathrm{P}_{\mu\nu}(q)\Delta(q^2)$, we get

$$\sum_{i=1}^{2}(a_i)_{\mu\nu} = \lambda\Big\{\frac{1}{2}\int_k \Gamma^{\alpha\beta}_\mu\Delta^\mathrm{t}_{\alpha\rho}(k)\Delta^t_{\beta\sigma}(k+q)\mathbf{L}^{\rho\sigma}_\nu - \frac{9}{4}g_{\mu\nu}\int_k\Delta(k) + \int_k\Delta^\mathrm{t}_{\alpha\mu}(k)\frac{(k+q)_\beta}{(k+q)^2} \times[\Gamma+\mathbf{L}]^{\alpha\beta}_\nu + \int_k\frac{k_\mu(k+q)_\nu}{k^2(k+q)^2}\Big\}, \quad (5)$$

where $\mathbf{L}_{\mu\alpha\beta} = \Gamma_{\mu\alpha\beta} + \mathbf{K}_{\mu\alpha\beta}$ satisfies the WI $q^\mu\mathbf{L}_{\mu\alpha\beta} = \mathrm{P}_{\alpha\beta}(k+q)\Delta^{-1}(k+q) - \mathrm{P}_{\alpha\beta}(k)\Delta^{-1}(k)$. Contracting the

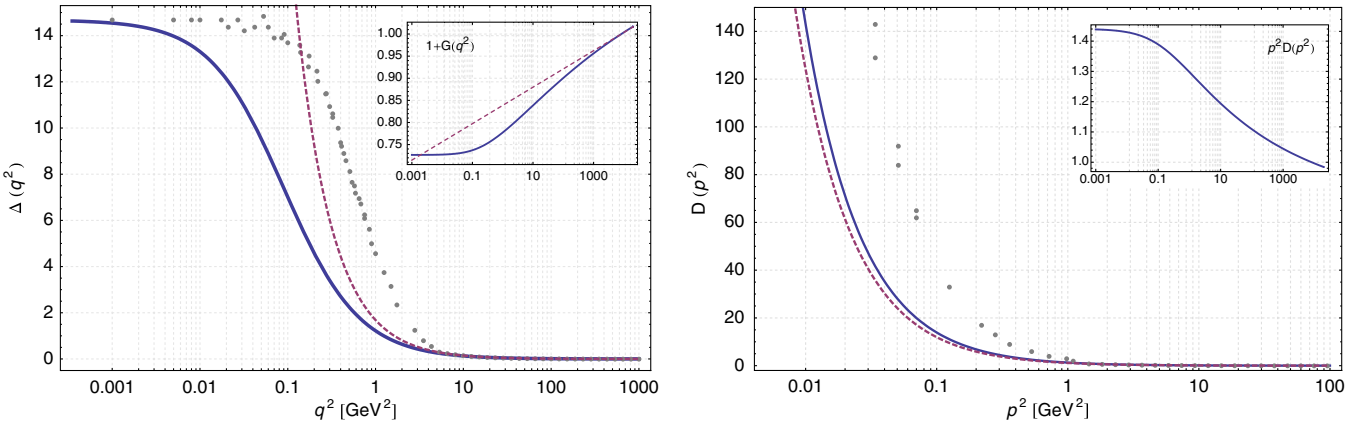

FIG. 2 (color online). Left panel: The gluon propagator obtained from the solution of the SDE system (blue continuous line) compared to the lattice data of [7]; the red dashed line represents the perturbative behavior. In the inset we show the function $1 + G(q^2)$ (blue continuous line) and its perturbative behavior (red dashed line). Right panel: The ghost propagator obtained from the SDE system (blue continuous line), the one-loop perturbative result (red dashed line), and the corresponding lattice data of [7]. In the inset we show the function $p^2D(p^2)$ from the SDE.

left-hand side (lhs) of (5) by q^μ one can then verify that it vanishes, as announced.

Next, following standard techniques, we express $\mathbf{L}_{\mu\alpha\beta}$ and $\tilde{\mathbf{\Gamma}}_\mu$ as a function of the gluon and ghost self-energy, respectively, in such a way as to automatically satisfy the corresponding WIs. Of course, this method leaves the transverse (i.e., identically conserved) part of the vertex undetermined. The ansatz we will use is

$$\begin{aligned} \mathbf{L}_{\mu\alpha\beta} &= \Gamma_{\mu\alpha\beta} + i\frac{q_\mu}{q^2}[\Pi_{\alpha\beta}(k+q) - \Pi_{\alpha\beta}(k)], \\ \tilde{\mathbf{\Gamma}}_\mu &= \tilde{\Gamma}_\mu - i\frac{q_\mu}{q^2}[L(k+q) - L(k)], \end{aligned} \tag{6}$$

whose essential feature is the presence of massless pole terms, $1/q^2$. Longitudinally coupled bound-state poles are known to be instrumental for obtaining $\Delta^{-1}(0) \neq 0$ [15]; on the other hand, due to current conservation, they do not contribute to the S-matrix. For the conventional ghost-gluon vertex $\mathbf{\Gamma}_\nu$, appearing in the second SDE of (2) we will use its tree-level expression, i.e., $\mathbf{\Gamma}_\nu \to \Gamma_\nu = -p_\nu$. Note that, unlike $\tilde{\mathbf{\Gamma}}_\nu$, the conventional $\mathbf{\Gamma}_\nu$ satisfies a STI of rather limited usefulness; the ability to employ such a different treatment for $\tilde{\mathbf{\Gamma}}_\nu$ and $\mathbf{\Gamma}_\nu$ without compromising gauge invariance is indicative of the versatility of the new SD formalism used here. Finally, for $H_{\sigma\nu}$ we use its tree-level value, $H^{(0)}_{\sigma\nu}$.

With these approximations, the last two equations of (2), together with (4) and (5), give (in Euclidean space)

$$\begin{aligned} [1+G(q^2)]^2\Delta^{-1}(q^2) &= q^2 - \frac{\lambda}{6}\Big[\int_k \Delta(k)\Delta(k+q)f_1 + \int_k \Delta(k)f_2 - \frac{1}{2}\int_k \frac{q^2}{k^2(k+q)^2}\Big] \\ &\quad + \lambda\Big[\frac{4}{3}\int_k\Big[k^2 - \frac{(k\cdot q)^2}{q^2}\Big]D(k)D(k+q) - 2\int_k D(k)\Big], \\ f_1 &= 20q^2 + 18k^2 - 6(k+q)^2 + \frac{(q^2)^2}{(k+q)^2} - (k\cdot q)^2\Big[\frac{20}{k^2} + \frac{10}{q^2} + \frac{q^2}{k^2(k+q)^2} + \frac{2(k+q)^2}{q^2k^2}\Big], \\ f_2 &= -\frac{27}{2} - 8\frac{k^2}{(k+q)^2} + 8\frac{q^2}{(k+q)^2} + 4\frac{(k\cdot q)^2}{k^2(k+q)^2} - 4\frac{(k\cdot q)^2}{q^2(k+q)^2}, \end{aligned} \tag{7}$$

$$\begin{aligned} D^{-1}(p^2) &= p^2 - \lambda\int_k\Big[p^2 - \frac{(p\cdot k)^2}{k^2}\Big]\Delta(k)D(p+k), \\ G(q^2) &= -\frac{\lambda}{3}\int_k\Big[2 + \frac{(k\cdot q)^2}{k^2q^2}\Big]\Delta(k)D(k+q). \end{aligned} \tag{8}$$

Since $[(a_1)+(a_2)]_{\mu\nu}$ and $[(a_3)+(a_4)]_{\mu\nu}$ are transverse, in arriving at (7) we have used $[(a_1)+(a_2)]_{\mu\nu} = \mathrm{Tr}[(a_1)+(a_2)]\mathrm{P}_{\mu\nu}(q)$ and $[(a_3)+(a_4)]_{\mu\nu} = \mathrm{Tr}[(a_3)+(a_4)]\mathrm{P}_{\mu\nu}(q)$, substituted into (2), and then equated the scalar cofactors of both sides. Thus, the transversality of the answer cannot be possibly compromised by the ensuing numerical treatment (e.g.

hard ultraviolet cutoffs), which may only affect the value of the cofactor.

III. NUMERICAL RESULTS

Before solving numerically the above system of integral equations, one must introduce renormalization constants to make them finite. The values of these constants will be fixed by the conditions $\Delta^{-1}(\mu^2) = \mu^2$, $D^{-1}(\mu^2) = \mu^2$, and $G(\mu^2) = 0$, with the renormalization point μ^2 of the order of M_Z^2. It is relatively straightforward to verify that the perturbative expansion of (7) and (8) furnishes the correct one-loop results. Specifically, keeping only leading logs, we have $1 + G(q^2) = 1 + \frac{3C_A\alpha_s}{16\pi}\ln(q^2/\mu^2)$, while $D^{-1}(p^2) = p^2[1 + \frac{3C_A\alpha_s}{16\pi}\ln(p^2/\mu^2)]$ and $\Delta^{-1}(q^2) = q^2[1 + \frac{13C_A\alpha_s}{24\pi}\ln(q^2/\mu^2)]$, where $\alpha_s = g^2/4\pi$.

The crux of the matter, however, is the behavior of (7) as $q^2 \to 0$, where the "freezing" of the gluon propagator is observed. In this limit, Eq. (7) yields

$$\Delta^{-1}(0) = \frac{\lambda(T_g + T_c)}{[1 + G(0)]^2}, \tag{9}$$

$$T_g = \frac{15}{4}\int_k \Delta(k) - \frac{3}{2}\int_k k^2\Delta^2(k), \tag{10}$$

$$T_c = -2\int_k D(k) + \int_k k^2 D^2(k). \tag{11}$$

Perturbatively the rhs of Eq. (9) vanishes by virtue of the dimensional regularization result $\int_k \frac{\ln^n k^2}{k^2} = 0$ $n = 0, 1, 2, \ldots$ which ensures the masslessness of the gluon to all orders. However, nonperturbatively $\Delta^{-1}(0)$ does *not* have to vanish, provided that the quadratically divergent integrals defining it can be properly regulated and made finite, *without* introducing counterterms of the form $m_0^2(\Lambda_{\rm UV}^2)A_\mu^2$, which are forbidden by the local gauge invariance of the fundamental QCD Lagrangian. It turns out that this is indeed possible: the divergent integrals can be regulated by subtracting appropriate combinations of "dimensional regularization zeros." Specifically, as we have verified explicitly and as can be clearly seen in Fig. 2 (left panel), for large enough k^2 the $\Delta(k^2)$ goes over to its perturbative expression, to be denoted by $\Delta_{\rm pert}(k^2)$; it has the form $\Delta_{\rm pert}(k^2) = \sum_{n=0}^{N} a_n \frac{\ln^n k^2}{k^2}$, where the coefficient a_n is known from the perturbative expansion. For the case at hand, measuring k^2 in GeV^2, using $\mu \approx 100$ GeV and $\alpha_s(\mu) = 0.1$, after inverting and reexpanding the $\Delta^{-1}(k^2)$ given below Eq. (8), we find $a_0 \approx 1.7$, $a_1 \approx -0.1$, $a_2 \approx 2.5 \times 10^{-3}$. Then, subtracting $\int_k \Delta_{\rm pert}(k^2) = 0$ from both sides of Eq. (10), we obtain the regularized $T_g^{\rm reg}$ given by ($k^2 = y$)

$$16\pi^2 T_g^{\rm reg} = \frac{15}{4}\int_0^s dy y[\Delta(y) - \Delta_{\rm pert}(y)] - \frac{3}{2}\int_0^s dy y^2[\Delta^2(y) - \Delta_{\rm pert}^2(y)]. \tag{12}$$

A similar procedure can be followed for T_c (see below). The obvious ambiguity of the regularization described above is the choice of the point s, past which the two curves, $\Delta(y)$ and $\Delta_{\rm pert}(y)$, are assumed to coincide.

Ideally, one should then: (i) solve the system of integral equations under the boundary condition $\Delta(0) = C$, where C is an arbitrary positive parameter; (ii) substitute the solutions for $\Delta(q)$ and $D(q)$ in the (regularized) integrals on the rhs of (9), together with the obtained value for $G(0)$, and denote the result by $\Delta_{\rm reg}^{-1}(0)$; (iii) check that the self-consistency requirement $\Delta_{\rm reg}^{-1}(0) = C^{-1}$ is satisfied; if not, (iv) a new C must be chosen and the procedure repeated. In practice, due to the aforementioned ambiguity, we cannot pin down $\Delta(0)$ completely, and we will restrict ourselves to providing a reasonable range for its value.

We have solved the system for a variety of initial values for C, ranging between 1–50 GeV^{-2}, and obtained from (12) the corresponding $\Delta_{\rm reg}^{-1}(0)$. On physical grounds one does not expect the perturbative expression $\Delta_{\rm pert}(k^2)$ to hold below 5–10 GeV^2, and therefore, when computing $\Delta_{\rm reg}^{-1}(0)$, s should be chosen around that value. For values of C between 10–25 GeV^{-2} the corresponding $\Delta_{\rm reg}^{-1}(0)$ can be made equal to C^{-1} by choosing values for s within that (physically reasonable) range. For example, for $C = 14.7$ GeV^{-2}, the value of the lattice data at the origin, we must choose $s \approx 10$ GeV^2. The solutions for $\Delta(q)$, $D(p)$, and $1 + G(q)$ obtained for that special choice, $C = 14.7$ GeV^{-2}, are shown in Fig. 2. In order to enforce the equality $\Delta_{\rm reg}^{-1}(0) = C^{-1}$ for higher values of C one must assume the validity of perturbation theory uncomfortably deep into the infrared region; for example, for $C = 50$ GeV^{-2} one must choose s below 1 GeV^2. We emphasize that the nonperturbative transverse gluon propagator, being finite in the IR, is automatically less singular than a simple pole, thus satisfying the corresponding Kugo-Ojima (KO) confinement criterion [16], essential for ensuring an unbroken color charge in QCD [17]. Note that for $q^2 \leq 10$ GeV^2 both gluon propagators (lattice and SDE) shown in Fig. 2 may be fitted very accurately using a unique functional form, given by $\Delta^{-1}(q^2) = a + b(q^2)^{c-1}$. Specifically [measuring q^2 in GeV^2 and the χ^2 per degrees of freedom], the lattice data are fitted by $a = 0.07$, $b = 0.15$, and $c = 2.54$ ($\chi^2 \sim 10^{-2}$), while our SDE solution is described setting $a = 0.07$, $b = 0.77$, and $c = 2.01$ ($\chi^2 \sim 10^{-4}$).

Let us now consider the ghosts. The $D(p^2)$ obtained from the ghost SDE diverges at the origin, in qualitative agreement with the lattice data. From the SDE point of view, this divergent behavior is due to the fact that we are working in the LG and the vertex $\mathbf{\Gamma}_\nu$ employed contains no

$1/p^2$ poles, as suggested by previous lattice studies [18]. The rate of divergence of our solution is particularly interesting, because it is related to the KO confinement criterion for the ghost [16], according to which the nonperturbative ghost propagator (in the LG) should be more singular in the infrared than a simple pole. Motivated by this, we proceed to fit the function $p^2D(p^2)$ [see inset in right panel of Fig. 2]. First we use a fitting function of the form $p^2D(p^2) = c_1(p^2)^{-\gamma}$ (p^2 in GeV^2); a positive γ would indicate that the SDE solution satisfies the KO criterion. Our best fit, valid for $p^2 \leq 10$, gives the values $\gamma = 0.02$ and $c_1 = 1.30$, which lead to a $\chi^2 \sim 10^{-3}$. Interestingly enough, an even better fit may be obtained using a qualitatively different, physically motivated functional form, namely $p^2D(p^2) = \kappa_1 - \kappa_2 \ln(p^2 + \kappa_3)$ (with κ_3 acting as a gluon ''mass''). Our best fit, valid for the same range, gives $\kappa_1 = 1.3$, $\kappa_2 = 0.05$, and $\kappa_3 = 0.05$, with $\chi^2 \sim 10^{-6}$. This second fit suggests that $p^2D(p^2)$ reaches a finite (positive) value as $p^2 \to 0$. Even though not conclusive, our fitting analysis seems to favor a ghost propagator displaying no power-law enhancement, in agreement with recent results presented in [19]; clearly, this question deserves further study.

Turning to the tadpole contributions T_c of (11), the subtraction of $0 = \int_k k^{-2}$ regularizes T_c, yielding a rather suppressed finite value for $T_c^{\rm reg}$. For example, using the first ghost fit, we get ($s' \approx 1$ GeV^2)

$$16\pi^2 T_c^{\rm reg} = -2\int_0^{s'} dy[yD(y) - 1] + \int_0^{s'} dy[y^2D^2(y) - 1] \sim -2\gamma^2 s' \ln s', \tag{13}$$

which is numerically negligible.

IV. DISCUSSION

The present work has focused on the derivation of an infrared finite gluon propagator from a gauge-invariant set of SDEs for pure QCD in the LG, and its comparison with recent lattice data. Following the classic works of [15], the finiteness of the gluon propagator is obtained by introducing massless poles in the corresponding three-gluon vertex. The actual value of $\Delta_{\rm reg}^{-1}(0)$ has been treated as a free parameter and was chosen to coincide with the lattice point at the origin. The curves shown in Fig. 2 were then obtained dynamically, from the solution of the SDE system, for the entire range of momenta. Comparing the solution for the gluon propagator with the lattice data we see that, whereas their asymptotic behavior coincides (perturbative limits), there is a discrepancy of about a factor of 2–2.5 in the intermediate region of momenta, especially around the fundamental QCD mass scale [reflected also in the different values of the two sets of fitting parameters (a, b, c)]. In the case of the ghost propagator the relative difference increases as one approaches the deep infrared, given that both curves diverge at a different rate. These discrepancies may be accounted for by extending the gluon SDE to include the ''two-loop dressed'' graphs, omitted (gauge invariantly) from the present analysis, and/or by supplying the relevant transverse parts of the vertex given in (6). We hope to be able to make progress in this direction in the near future.

In our opinion, the analysis presented here, in conjunction with the recent lattice data, fully corroborates Cornwall's early description of QCD in terms of a dynamically generated, momentum-dependent gluon mass [9]. In this picture the low-energy effective theory of QCD is a nonlinear sigma model, known as massive gauge-invariant Yang-Mills theory, obtained from the generalization of Stückelberg's construction to non-Abelian theories [20]. This model admits vortex solutions, with a long-range pure gauge term in their potentials, which endows them with a topological quantum number corresponding to the center of the gauge group [Z_N for $SU(N)$], and is, in turn, responsible for quark confinement and gluon screening [21,22]. Specifically, center vortices of thickness $\sim m^{-1}$, where m is the induced mass of the gluon, form a condensate because their entropy (per unit size) is larger than their action. This condensation furnishes an area law to the fundamental representation Wilson loop, thus confining quarks. On the other hand, the adjoint potential shows a roughly linear regime followed by string breaking when the potential energy is about $2m$, corresponding to gluon screening [23].

ACKNOWLEDGMENTS

Work supported by the Spanish MEC Grants No. FPA 2005-01678 and No. FPA 2005-00711, and the Fundación General of the UV. We thank Professor J. M. Cornwall for several useful comments.

[1] W. J. Marciano and H. Pagels, Phys. Rep. **36**, 137 (1978).
[2] See, for example, J. Greensite, Prog. Part. Nucl. Phys. **51**, 1 (2003), and references therein.
[3] F. J. Dyson, Phys. Rev. **75**, 1736 (1949).
[4] J. S. Schwinger, Proc. Natl. Acad. Sci. U.S.A. **37**, 452 (1951); **37**, 455 (1951).
[5] J. D. Bjorken and S. D. Drell, Relativistic Quantum Field Theory, Chap. 19; C. Itzykson and J. B. Zuber, Quantum Field Theory, Chap. 10.
[6] A. Cucchieri and T. Mendes, Proc. Sci., LATTICE2007 (2007) 297; P. O. Bowman *et al.*, Phys. Rev. D **76**, 094505 (2007).

[7] I. L. Bogolubsky *et al.*, Proc. Sci., LATTICE2007 (2007) 290.
[8] A. G. Williams, Prog. Theor. Phys. Suppl. **151**, 154 (2003); A. Sternbeck *et al.*, AIP Conf. Proc. **756**, 284 (2005); P. J. Silva and O. Oliveira, Nucl. Phys. **B690**, 177 (2004).
[9] J. M. Cornwall, Phys. Rev. D **26**, 1453 (1982).
[10] D. Binosi and J. Papavassiliou, Phys. Rev. D **77**, 061702 (2008).
[11] J. M. Cornwall and J. Papavassiliou, Phys. Rev. D **40**, 3474 (1989).
[12] D. Binosi and J. Papavassiliou, Phys. Rev. D **66**, 025024 (2002); **66**, 111901 (2002); J. Phys. G **30**, 203 (2004); A. Pilaftsis, Nucl. Phys. **B487**, 467 (1997).
[13] L. F. Abbott, Nucl. Phys. **B185**, 189 (1981).
[14] A. C. Aguilar and J. Papavassiliou, J. High Energy Phys. 12 (2006) 012.
[15] R. Jackiw and K. Johnson, Phys. Rev. D **8**, 2386 (1973); J. M. Cornwall and R. E. Norton, Phys. Rev. D **8**, 3338 (1973); E. Eichten and F. Feinberg, Phys. Rev. D **10**, 3254 (1974).
[16] T. Kugo and I. Ojima, Prog. Theor. Phys. Suppl. **66**, 1 (1979).
[17] See, e.g., C. S. Fischer, J. Phys. G **32**, R253 (2006), and references therein.
[18] A. Cucchieri, T. Mendes, and A. Mihara, J. High Energy Phys. 12 (2004) 012.
[19] Ph. Boucaud *et al.*, arXiv:0803.2161.
[20] J. M. Cornwall, Phys. Rev. D **10**, 500 (1974).
[21] J. M. Cornwall, Nucl. Phys. **B157**, 392 (1979).
[22] C. W. Bernard, Nucl. Phys. **B219**, 341 (1983).
[23] J. M. Cornwall, Phys. Rev. D **57**, 7589 (1998).